

The mechanism of the dextran-induced red blood cell aggregation

A. Pribush · D. Zilberman-Kravits ·
N. Meyerstein

Received: 30 May 2006 / Accepted: 10 October 2006 / Published online: 8 November 2006
© EBSA 2006

Abstract In order to clarify the mechanism of dextran-induced aggregation, the effect of the ionic strength (I) on the minimal shear stress (τ_c) required to rupture RBC doublets was studied for suspensions with the external media containing 76 and 298 kDa dextrans. At low and high ionic strengths, τ_c increases with increasing I , whereas at intermediate I values, τ_c versus I dependencies reveal a plateau step. The non-monotonous shape of these curves disagrees with the depletion model of RBC aggregation and is consistent with the predictions of the bridging mechanism. Literature reports point out that elastic behavior of dextran molecules in low and high I regions is fairly typical of Hookean springs and hence predict an increase in τ_c with increasing I . A plateau step is accounted for by the enthalpic component of the dextran elasticity due to the shear-induced chair–boat transition of the dextran’s glucopyranose rings. A longer plateau step for suspensions with a higher molecular weight dextran is explained by a larger contribution of the enthalpic component to the dextran elasticity. Thus, the results reported in this study provide evidence that RBC aggregation is caused by the formation of dextran bridges between the cells.

Keywords Erythrocyte aggregation · Bridging · Depletion layer models

Introduction

Problem statement

Although dextrans are not constituents of blood plasma, external media containing these polysaccharides are widely used to elucidate basic and applied aspects of blood rheological and transport properties. A broad application of these artificial aggregating media is motivated by the ability of dextrans to promote the formation of RBC aggregates with different morphology and size: depending on the molecular weight (MW) and concentration of dextrans, RBC aggregate morphology varies from short linear rouleaux to continuous RBC network. Significant efforts have been applied to elucidate the mechanism of dextran-induced RBC aggregation. However, despite these efforts, this mechanism still remains a controversial issue.

Findings that RBC aggregation (Brooks 1973c; Barshtein et al. 1998; Neu and Meiselman 2002; Pribush et al. 2000) and electrophoretic mobility (EM) (Bäumler et al. 1999, 2001; Brooks 1973a, b, c; Neu and Meiselman 2002; Neu et al. 2003) are affected by dextrans, suggest that the dextran concentration and electrical potential profiles near the interface membrane/continuous phase are important determinants of these phenomena. Therefore, it seemed logical to use RBC EM data with the aim to extract information concerning the mechanism of RBC aggregation. Attempts to understand why RBC electrophoretic mobilities in dextran containing solutions are higher

A. Pribush (✉) · D. Zilberman-Kravits · N. Meyerstein
Experimental Hematology Laboratory,
Physiology Department, Faculty of Health Sciences,
Ben-Gurion University of the Negev,
Beer-Sheva 84105, Israel
e-mail: alexp@bgumail.bgu.ac.il

A. Pribush
Chemistry Department, Faculty of Natural Sciences,
Ben-Gurion University of the Negev,
Beer-Sheva, Israel

than those predicted by the von Smoluchowski equation, fall into two groups:

1. Results obtained with the use of tritium- (Brooks 1973b; Chien et al. 1977) and fluorescently- (Alvarez et al. 1996) labeled dextrans, electron microscopic observations of RBCs in dextran containing solutions (Cudd et al. 1989) and dextran-induced changes in surface undulations of erythrocytes (Fricke et al. 1986) provided arguments for a high affinity of these polysaccharides for the membrane surface. Based on these experimental results, it was assumed that the dextran adsorption onto RBC surface changes the chemical potential of ions in the diffuse part of electrical double layer (EDL) thereby increasing RBC ζ -potential (Brooks 1973a). The bell-shaped dependence of RBC aggregation on the concentration of dextrans was accounted for by a dextran-dependent balance between electrostatic repulsion of EDLs and intercellular bridging (Brooks 1973c).
2. Alternative interpretation of dextran-induced changes in RBC EM (Bäumler et al. 1999, 2001; Neu and Meiselman 2002; Neu et al. 2003) led to the formulation of the depletion layer mechanism of RBC aggregation. It was assumed that an increase in the configurational entropy of dextrans near the interface is not balanced by adsorption energy. As the result of this imbalance, the dextran concentration and hence the viscosity near RBC membrane increase with a distance from the interface and these changes are manifested by an enhanced RBC EM. It was concluded that a reduced dextran concentration in the gap between two neighboring RBCs creates a pressure deficit and leads to an attraction between the cells (Bäumler et al. 1999, 2001; Neu and Meiselman 2002; Neu et al. 2003).

Thus, depending on a theoretical model used to explain an increase in RBC EM in the presence of dextrans, two mutually exclusive mechanisms for RBC aggregation—the bridging and depletion layer models were proposed. It should be noted that though extensive efforts were applied to provide insight into the electrokinetic behavior of biological cells [e.g., (Donath and Voigt 1986; Hsu et al. 2003; Haydon and Seaman 1967; de Kerchove and Elimelech 2005; Levine et al. 1983; Ohshima 2000)], complicated physical and physicochemical problems posed by electrophoresis of non-spherical, soft particles covered by non-homogeneously charged, ion-penetrable frictional layer the thickness of which is comparable with the Debye screening length, are not yet exactly solved. For this

reason, these conflicting interpretations of the enhanced RBC EM in the presence of dextrans are essentially based on simplifications and assumptions.

Another problem is associated with the reliability of dextran adsorption data. Results reported in a number of studies (Baskurt et al. 2002; Brooks et al. 1980; Rampling 1988) cast doubts on an effective adsorption of dextrans onto RBC membrane (Alvarez et al. 1996; Brooks 1973b; Chien et al. 1977; Cudd et al. 1989). Thus, given that arguments both for and against each of these aggregation models are disputable, neither the bridging nor depletion mechanism can be either accepted or refuted. It becomes clear that other approaches are required to elucidate the mechanism of the dextran-induced RBC aggregation.

Rationale for the study

The bridging and depletion flocculation models differ in many aspects. One of them is that these models predict qualitatively different dependencies of the fracture energy (Γ) on the ionic strength (I). Provided that RBCs interact via the depletion mechanism, the magnitude of Γ is determined by a combination of the electrostatic double layer and depletion interactions (Bäumler et al. 1999, 2001; Neu et al. 2003). A decrease in the ionic strength increases the intensity of electrostatic repulsion and hence enlarges the intermembrane distance between RBCs in aggregates. At first approximation, distance (D) dependencies of energies of the above mentioned interactions for separation distances larger than one Debye length are either an exponential function (electrostatic repulsion) or scale to D^{-n} (depletion attraction). Since the intensities of these interactions decay monotonically with the intermembrane separation, the fracture energy should gradually decrease with a decrease in the ionic strength approaching the thermal energy at sufficiently low I values. This conclusion is supported by the reported results (Neu et al. 2003) showing that the sum of the electrostatic and depletion interaction energies is a linearly decreasing function of the Debye length.

If RBCs interact via the formation of dextran bridges, a Γ versus I dependence is expected to be qualitatively different. The energy required to rupture dextran bridges is spent for stretching of elastic dextran molecules (E_{el}) and their detachment from the membrane (E_{det}). One may assume that the binding of dextrans to the membrane is mainly caused by hydrogen and van der Waals interactions and therefore should be minimally affected by the ionic strength. Findings that the dextran adsorption isotherms are unaffected by ionic strength (Brooks 1973b, c),

corroborate this assumption. Since effects of I on the dextran surface concentration and the binding energy may be ignored, it may be concluded that whether or not $\Gamma(I)$ is a monotonous function, depends solely on a E_{el} versus I dependence. In other words, a shape of $\Gamma(I)$ dependence should be controlled by the elasticity of dextran molecules.

Recent advances in atomic force microscopy (AFM) enabled detailed investigations of this issue. It was shown that in the low-force regime, dextrans act as a linear spring. A plateau step (Li et al. 1999; Marszalek et al. 1998; Rief et al. 1998) or a significant decrease in the slope of force-extension curves (Rief et al. 1997) at higher forces are accounted for by the chair–boat transition of glucopyranose rings of dextran molecules.¹ Further small force-induced stretching is due to deformation of the rings in the boat-like conformation and bending the glycosidic linkages. Finally, when the maximum binding force is exceeded, the molecule ruptures from the AFM probe tip. These AFM data allow the following predictions: 1. In high and low I regions when the intermembrane separation is small and large, elastic behavior of bridging dextran molecules is fairly typical of Hookean springs. 2. At intermediate ionic strengths, either E_{el} remains unchanged or the slope of $E_{el}(I)$ curves should be substantially smaller than that in low and high I regions.

Neglecting electrodynamic interactions, the total energy of the bridging interaction is the sum of E_{Coul} , E_{st} , E_{el} and E_{det} , where E_{Coul} and E_{st} are the energies of electrostatic and steric interactions. Since a distance dependence of E_{st} scales to D^{-n} (Helfrich 1978), it is reasonable to assume that E_{st} is a monotonous function of I . A superposition of non-monotonous $E_{el}(I)$, monotonous $E_{Coul}(I)$ and $E_{st}(I)$ functions and E_{det} , which as has been shown above is unaffected by I , yields a non-monotonous dependence. Therefore, if RBCs interact via the formation of dextran bridges, a shape of $\Gamma(I)$ curves is expected to be as follows: in low and high I regions, Γ should increase with increasing ionic strength, whereas either a significantly smaller slope of $\Gamma(I)$ curves or a plateau step is expected to be at intermediate ionic strengths.

Thus, the above analysis points out that the ionic strength may be used as an appropriate control parameter with which to clarify the mechanism of dextran-induced RBC aggregation. It should be noted that this approach is based on the most general, qualitative predictions of the bridging and depletion layer flocculation models and therefore avoids unre-

solved problems associated with a quantitative analysis of Derjaguin, Landau, Verwey and Overbeek (DLVO) and non-DLVO forces between non-uniformly charged, non-spherical, deformable RBCs covered by glycocalyx and adsorbed neutral polymers. Another advantage of this approach is that, it does not require the application of disputable dextran adsorption data.

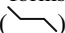
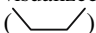
Materials and methods

RBC suspensions

Blood units, within seven days after donation, were supplied by the blood bank of the Soroka University Medical Center (Beer-Sheva, Israel). Literature reports point out that RBC deformability (Raat et al. 2005), aggregability (Hovav et al. 1999), morphology of cells (Berezina et al. 2002), mean corpuscular volume (Cicha et al. 2000) and the surface charge density of RBC membrane (Godin and Caprani 1997) do not reveal measurable changes during storage of blood up to ~10 days. Studies were performed with RBCs suspended in external media containing the following dextrans: 40 kDa at 15 and 30 g/l; 76 kDa at 23 g/l; 80 kDa at 15 and 30 g/l; 298 kDa at 10, 15 and 30 g/l and 2,000 kDa at 5 g/l. Molecular weights of dextrans were supplied by the vendor (Sigma, St. Louis, MO, USA); hereinafter, these dextrans are termed D40, D76, D80, D298 and D2,000, respectively.

The ionic strength of aggregating media was varied by changes in the fraction of the isoosmotic low ionic strength solution (LIS; $I = 0.036$ M) in saline ($I = 0.154$ M); LIS: 30.8 mM NaCl, 1.5 mM Na_2HPO_4 , 1.5 mM NaH_2PO_4 and 240 mM glycine; pH 6.7. The effect of the ionic strength on RBC aggregate break-up was studied for suspensions with the external media containing D76 (23 g/l) and D298 (10 g/l). pH of external media used in this study varied from 5.7 (saline) to 6.7 (LIS). Changes in pH in this range do not affect both RBC EM (Haydon and Seaman 1967) and aggregation (Maeda et al. 1988).

RBC suspensions were prepared using the following protocol: (1) plasma and buffy coat were removed by aspiration after centrifugation for 10 min at ~300 g; (2) RBCs were then washed once with an appropriate external medium and finally re-suspended at Hct = 0.45 v/v. Hematocrit was determined using a micro-centrifuge (Hematocrit KH-1200 M, Kubota, Japan). Measurements were carried out within ~2 h after suspensions were prepared. Microscopic observations performed within this time, did not reveal changes in RBC morphology.

¹ These two forms may be visualized as follows (Fisher et al. 1999): chair () → boat (.

Qualitatively, experimental results obtained for suspensions prepared from eight blood units were well reproducible, though quantitatively a certain sample-to-sample variation was observed. Therefore, results shown in each figure were obtained for suspension(s) prepared from the same blood unit.

Measurements of the conductance and capacitance

The experimental part of this study is essentially based on our prior results which showed that the capacitance measured at a frequency (0.2 MHz) far below the midpoint of the β -dispersion is proportional to the mean effective size of the dispersed particles (Pribush et al. 1999, 2000) whereas the time-dependent conductance follows morphological evolutions of RBC aggregates (Pribush et al. 2004a).

The technique of measuring the passive and active components of the blood admittance has been previously described in full detail (Pribush et al. 1999, 2004a). In brief, the measurements were carried out for the parallel circuit mode using a precision LCR meter (HP 4285A) equipped with a test fixture (HP 16047A, Yokogawa Hewlett-Packard, Tokyo, Japan). A low voltage test signal (10 mV) was employed in order to minimize the current density; the time interval between two measurements was ~ 200 ms. Raw experimental data were converted to ASCII format and imported into a spreadsheet program. All measurements were under full computer control. The measured capacitance was corrected for the effects of the series inductance (2×10^{-7} H) and stray capacitance (2.5 pF). Time-dependent changes in the admittance of the same RBC suspension at a certain flow condition were subsequently recorded 4–5 times. Standard error of mean steady-state capacitance values determined from these measurements did not exceed $\pm 0.8\%$. All measurements were made at room temperature ($24 \pm 1^\circ\text{C}$).

In the general case, time-dependent changes in the active and passive components of blood admittance recorded after a sudden increase in flow velocity are affected by both a dispersion of RBC aggregates (Pribush et al. 1999, 2004a) and migration-induced changes in the cross-stream Hct distribution (Pribush et al. 2004b). The former process is completed in less than 15–20 s, whereas a very small traveling distance of RBC aggregates during this time does not affect measurably the cross-stream Hct profile (Pribush et al. 2004b). Thus, time dependencies of conductance (G) and capacitance (C) signals recorded during ~ 15 –20 s after a sudden increase in shear rate are not affected by the inward migration of individual RBCs and their aggregates.

Flow conditions

The square inner cross-section (2×2 mm) chamber fabricated from Plexiglas was fitted with two opposing 2 mm diameter Ag/AgCl electrodes (INV Co., CA, USA). Reported results obtained for 2 and 6 mm thick chambers (Pribush et al. 2000) indicate that the 2 mm thick chamber is large enough to ignore effects of cell-wall interactions on the blood admittance. Note also that the Fåhræus effect (Fåhræus 1929) is negligible for 2 mm thick flow channels (Cokelet 1999). The 20 cm long chamber was connected to a stepper motor-driven syringe pump (KDS 200, KD Scientific, MA, USA) which permitted the flow rate to be abruptly changed and to a blood reservoir by 2 mm inner diameter plastic tubings. As specified by the manufacturer, the typical accuracy of this particular syringe pump is $\pm 1\%$ or better. The electrodes were located at 1 cm from the end of the chamber. Unless otherwise indicated, measurements were performed when electrodes were located at 19 cm from the entrance. RBC suspensions were withdrawn by a syringe pump from a reservoir where they were constantly mixed with a magnetic stirrer (model F-13, Fried Electric, Haifa, Israel) in order to avoid sedimentation-induced changes in the feed Hct. The block-diagram of the setup and the sketch of the measuring chamber are shown in Fig. 1.

Ideally, flow conditions should be characterized by the cross-stream velocity distributions, which may be derived from the continuity, RBC transport and Navier–Stokes equations generalized to a certain non-Newtonian blood model. Unfortunately, attempts to use this approach face serious problems. First, since blood is usually treated as a shear-thinning fluid with a yield stress, it remains unclear which model of a shear-thinning fluid should be used. Note also that because of the formation of plasma layer near the walls, measurements of a yield stress are somewhat problematic. Second, recently, it has been shown that blood in low flow regime when RBCs form a network-like structure behaves as a dilatant fluid (Pribush et al. 2004b). Third, one of parameters of the RBC transport equation is the time-dependent cross-stream Hct profile. Unfortunately, current experimental methods suggested so far fail to determine the instantaneous cross-sectional Hct profile in relatively thick blood layers. Thus, because of the lack of reliable information required to compute cross-stream velocity profiles, severe simplifications and assumptions must be used. Obviously, these simplifications and assumptions will cast doubt on reliability of calculated cross-stream velocity profiles. Therefore, to quantify flow conditions, we used the

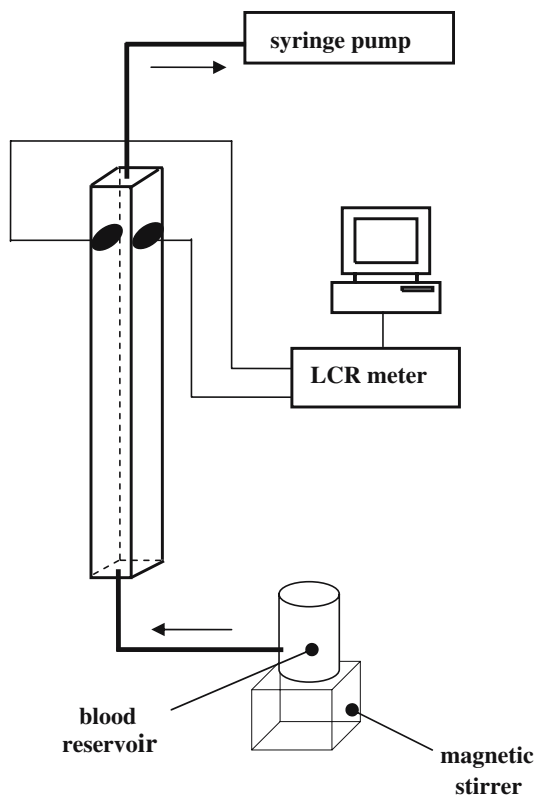


Fig. 1 The block-diagram of the setup and the sketch of the 20 cm long measuring chamber. The electrodes are located at 19.0 cm from the entrance of the chamber. Arrows indicate the direction of flow

average shear rates (hereafter called the shear rates, $\dot{\gamma}$), which were calculated from the cross-sectional geometry of the flowing chamber and the known net flow velocity.

The following experimental protocol was used: (1) RBC suspensions were sheared at 93.7 s^{-1} to completely disperse RBC aggregates; (2) the shear rate was reduced to a new level (termed the intermediate shear rate, $\dot{\gamma}_{\text{int}}$) and RBC aggregates were allowed to form; (3) then after G and C reached stationary levels, the flow velocity was increased to promote disaggregation. Vertical arrows in figures indicate changes in the shear rate.

Since, as mentioned above, blood flow in a tube is accompanied by the inward migration of RBCs, cross-stream Hct and velocity profiles change gradually along the measuring chamber. Therefore, if kinetics of the disaggregation process at the same net flow velocity are affected by the cross-sectional shear rate and hematocrit distributions, time dependencies of signals recorded after an abrupt increase in the net flow velocity will depend on the axial position. To clarify if that is the case, time-dependent conductance and

capacitance of the same suspension were recorded at 1.0 and 19.0 cm from the entrance of the chamber. Comparison of C signals (Fig. 2) does not reveal a marked effect of the axial position on kinetics of the aggregation and disaggregation processes.

To verify that the shear rate of 93.7 s^{-1} is high enough to fully disperse RBC aggregates formed in suspension with the stronger aggregating medium (saline-D298), the steady-state capacitance was recorded at the shear rates from 82.5 to 110 s^{-1} . It was found that the steady-state C in this range of $\dot{\gamma}$ remains unchanged. Given that the capacitance is proportional to the mean effective radius of the dispersed particles (Schwan 1963; Pribush et al. 1999), this finding suggests that the shear rate of 93.7 s^{-1} is sufficient for complete dispersion of aggregates.

Results

Dispersion of RBC aggregates in shear flow

In stasis and at low shear rates RBCs in suspensions with these particular dextrans (i.e., D76 and D298) form branched aggregates (Pribush et al. 2004a). Therefore, in order to avoid a need to consider both face-to-face and face-to-side intercellular links the strengths of which are essentially different (Pribush et al. 2000), the intermediate shear rates were suffi-

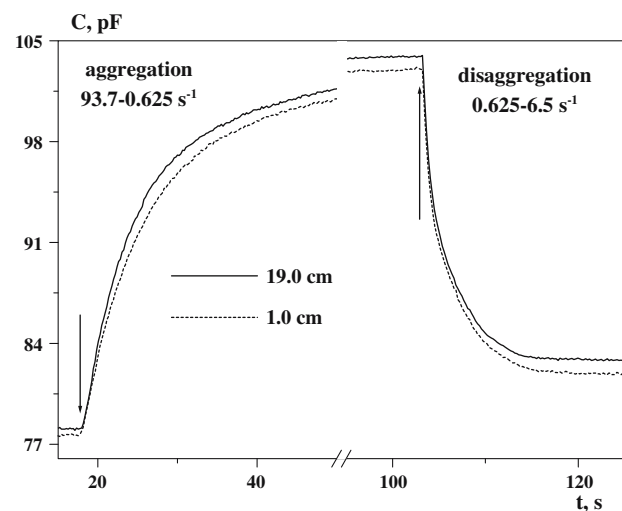


Fig. 2 Capacitance signals recorded for suspension prepared with the saline-D76 medium at 1.0 and 19.0 cm from the entrance. The following sequence of shear rates was utilized: (1) aggregates were completely dispersed at $\dot{\gamma} = 93.7 \text{ s}^{-1}$; (2) after C reached plateau levels, a low shear rate of 0.625 s^{-1} was applied to form aggregates; (3) when C reached steady-states, the shear rate was increased to 6.5 s^{-1} to promote disaggregation

ciently high to prevent the formation of branched aggregates. In accordance with our recent results (Pribush et al. 2004a), the similarity of shapes of $C(t)$ and $G(t)$ curves (Fig. 3) served as a criterion of the formation of linear rouleaux at a given intermediate shear rate.

A representative set of the capacitance kinetic curves recorded for suspension with the external medium consisting of equal fractions of saline and LIS ($I = 0.095$ M) is shown in Fig. 4. Given that the capacitance is proportional to the mean effective radius of the dispersed particles (Schwan 1963; Pribush et al. 1999), these curves reflect the kinetics of the disaggregation process and the steady-state effective radius of the aggregates, r_{Ag}^{eff} , at different final shear

rates, $\dot{\gamma}_{fin}$. Capacitance signals at different final shear rates were recorded for each ionic strength of the external media containing D76 and D298. These data were used to clarify the effect of the ionic strength on the fracture energy.

In order to determine the fracture energy or a parameter proportional to Γ , it is convenient to use the traditional method of floc strength characterization. Experimental (Sonntag and Russel 1986) and theoretical (Sonntag and Russel 1987) results obtained for disaggregation of flocs in the shear flow show that the steady-state floc size relates to the shear rate via a power law: $r_{Ag}^{eff} \sim \dot{\gamma}^{-m}$, where the exponent m is a function of the fractal dimension of flocs and their elasticity. However, this expression is applicable for very dilute colloidal suspensions when effects of dispersed particles and their interactions on the viscosity of suspensions may be ignored and hence, they behave as Newtonian liquids. At high volume fractions of dispersed phase, these effects cannot be ignored and therefore, suspensions behave as non-Newtonian fluids. In this case, the effect of shear rate-dependent viscosity of a suspension on the shear force acting aggregates becomes important. Therefore, it is not surprising that for blood and RBC suspensions ($Hct \geq 0.15$ v/v), it was found that $r_{Ag}^{eff} \sim (\eta\dot{\gamma})^{-m}$ (Snabre et al. 1987), where η is the viscosity of RBC suspension; (hereinafter, for brevity, the product of $\eta\dot{\gamma}$ is termed as the shear stress, τ).² Theoretical (Snabre et al. 1987) and experimental (Snabre et al. 1987, 2000) studies of RBC aggregate breakup corroborated the validity of this relationship for moderate and relatively low shear flows whereas in the region of high shear stresses, the logarithmic dependence of r_{Ag}^{eff} on the shear stress deviates from linearity approaching asymptotically the complete dispersion ($r_{Ag}^{eff} = r_{RBC}$). The minimal (critical) shear stress required to disperse RBC doublets ($\tau_c = F_d S$, where F_d and S are the disruption force and the contact surface area of interacting RBCs) was determined by extrapolating the linear portions of r_{Ag}^{eff} versus τ curves to the complete dispersion of the aggregates (Snabre et al. 2000). Using the Derjaguin's formula (Derjaguin et al. 1975), which relates the disruption force to the fracture energy ($F_d = 2\pi R\Gamma$, where R is the mean curvature radius of particles), one obtains that $\Gamma = \tau_c / 2\pi RS$. Therefore, given that $\tau \sim \eta\dot{\gamma}$ the viscosity of RBC suspensions at various shear rates must be determined.

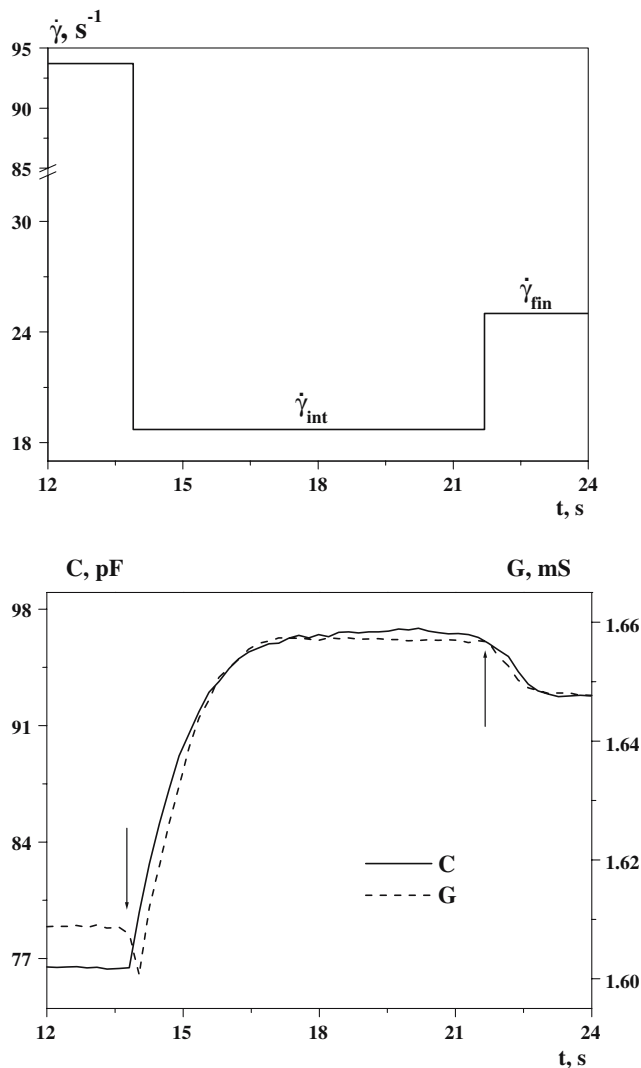


Fig. 3 Capacitance (solid line) and conductance (dashed line) signals recorded for suspension with the external media ($I = 0.154$ M) containing D298 (10 g/l). The timing diagram of the shear rate ($93.7 - 18.7 - 25.0$ s⁻¹) is shown in the upper panel

² Since blood is a yield stress material (Yeow et al 2002), its true shear stress differs from the product of $\eta\dot{\gamma}$.

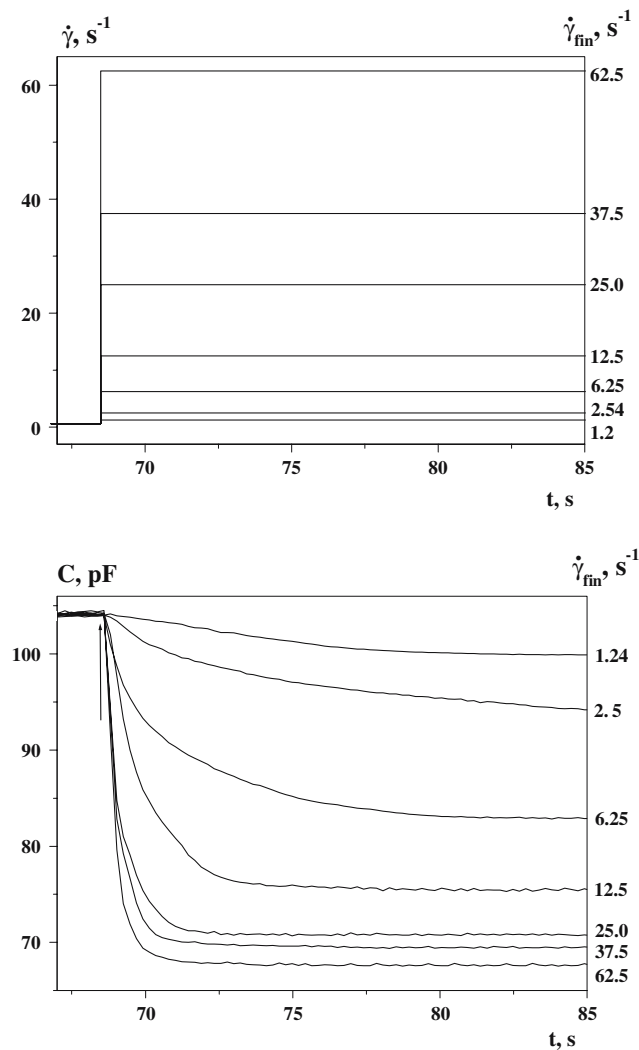


Fig. 4 The shear-induced kinetics of the aggregate break-up and timing diagrams of the shear rate (*upper panel*). In each test, RBC aggregates formed in the aggregating medium ($I = 0.095$ M) containing D76 (23 g/l) were initially dispersed at 93.7 s^{-1} and then the shear rate was reduced to 0.625 s^{-1} . After a plateau level of C was reached, the shear rate was increased to the values (in s^{-1}) shown in each panel

Shear viscosity of suspensions

Since a suitable viscometer was not available at Ben-Gurion University, we utilized the viscosity data that were kindly provided by Prof. H. J. Meiselman from the University of Southern California (CA, USA). However, these data might be used provided that variations of properties of RBCs taken from healthy individuals do not affect markedly the shear-dependent viscosity. Results reported in the literature gave an opportunity to clarify if this the case. Comparison of experimental data obtained by Merrill et al. (Merrill et al. 1965) and Goldsmith (Goldsmith 1974) for

control blood samples with Hct ~ 0.4 v/v shows that a shear stress versus shear rate dependence measured at shear rates from 1 to 100 s^{-1} is minimally affected by individual RBC and plasma properties. These data are in line with findings (Mi et al. 2004) that a viscosity versus shear rate dependence for blood samples taken from healthy individuals measured at $\dot{\gamma}$ from 10 to 110 s^{-1} is insignificantly affected by individual properties of blood. Thus, these findings suggest that shear viscosity data obtained in the laboratory of Prof. Meiselman may be used to interpret results of our study.

The steady-state viscosity of suspensions of RBCs (Hct = 0.45 v/v) in saline containing D40 (15 and 30 g/l), D80 (15 and 30 g/l), D250 (15 and 30 g/l) and D2,000 (5 g/l) was measured at shear rates from 0.08 to 95.0 s^{-1} . The following equations provide the best fit to these data:

$$\ln(\eta/\eta_m) = 1.885 - 0.116 \times \ln \dot{\gamma} \text{ (D40, 15 g/l)} \quad (1)$$

$$\ln(\eta/\eta_m) = 2.122 - 0.172 \times \ln \dot{\gamma} \text{ (D40, 30 g/l)} \quad (2)$$

$$\ln(\eta/\eta_m) = 2.797 - 0.367 \times \ln \dot{\gamma} \text{ (D80, 15 g/l)} \quad (3)$$

$$\ln(\eta/\eta_m) = 3.020 - 0.412 \times \ln \dot{\gamma} \text{ (D80, 30 g/l)} \quad (4)$$

$$\ln(\eta/\eta_m) = 2.570 - 0.311 \times \ln \dot{\gamma} \text{ (D250, 15 g/l)} \quad (5)$$

$$\ln(\eta/\eta_m) = 3.053 - 0.397 \times \ln \dot{\gamma} \text{ (D250, 30 g/l)} \quad (6)$$

$$\ln(\eta/\eta_m) = 2.654 - 0.345 \times \ln \dot{\gamma} \text{ (D2,000, 5 g/l)} \quad (7)$$

where η_m is the viscosity of the external media.

There are many factors to be taken into consideration when analyzing the shear-dependent viscosity of concentrated suspensions: the electrolyte and surfac-

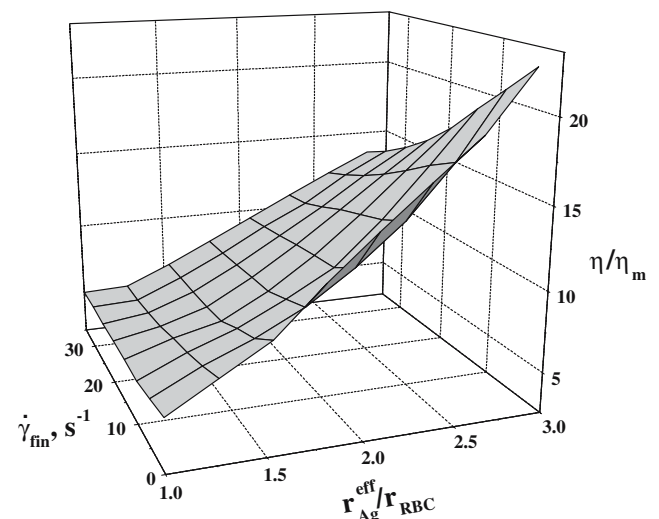
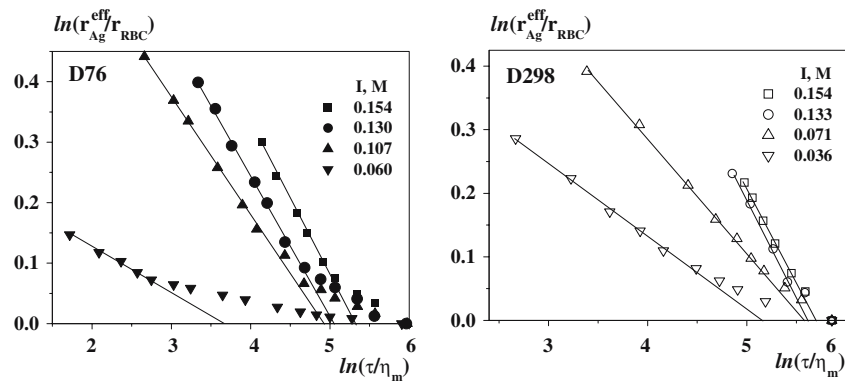


Fig. 5 The η/η_m versus $\dot{\gamma}_{fin}$ and r_{Ag}^{eff}/r_{RBC} dependence

Fig. 6 Representative $\ln(r_{\text{Ag}}^{\text{eff}}/r_{\text{RBC}})$ versus $\ln(\tau/\eta_m)$ dependencies for suspensions with the external media containing D76 (23 g/l) and D298 (10 g/l) at different ionic strengths. The values of the ionic strengths are shown in each panel



tant concentrations in the continuous phase, its viscosity, electroviscous effects, deformability of particles, their shape, size and volume fraction, the intensity of colloidal and hydrodynamic interparticle interactions. Depending on the specific properties of a disperse system and experimental conditions, each of these factors may play both a primary and secondary role. However, the reported data clearly indicate that the shear dependence of the blood viscosity in the range of the shear rates from ~ 0.05 to $\sim 40 \text{ s}^{-1}$ is mainly controlled by RBC aggregability (Thurston 1972). Since RBC aggregability may be quantified by the effective size of RBC aggregates (Pribush et al. 1999), one may suggest that at a constant Hct $\eta = f(r_{\text{Ag}}^{\text{eff}}/r_{\text{RBC}}, \dot{\gamma}_{\text{fin}}, \eta_m)$.

In accordance with theoretical models dealing with viscoelastic properties of disperse systems (Einstein 1906; Krieger and Dougherty 1959; Quemada 1977; Starov and Zhdanov 2003), it is suggested that η is proportional to η_m . Therefore, the expression for the viscosity of RBC suspensions may be simplified as follows: $\eta/\eta_m = \varphi(r_{\text{Ag}}^{\text{eff}}/r_{\text{RBC}}, \dot{\gamma}_{\text{fin}})$. The relative effective steady-state radii of RBC aggregates, $r_{\text{Ag}}^{\text{eff}}/r_{\text{RBC}}$, formed in suspensions with saline containing D40 (15 and 30 g/l), D80 (15 and 30 g/l), D298 (15 and 30 g/l) and D2,000 (5 g/l) at different final shear rates were calculated from the capacitance plateau levels ($r_{\text{Ag}}^{\text{st}}/r_{\text{RBC}} = C_{\dot{\gamma}_{\text{fin}_i}}/C_{93.7}$, where subscripts $\dot{\gamma}_{\text{fin}_i}$ and 93.7 designate the shear rate values; $\dot{\gamma}_{\text{fin}_i} \leq 93.7 \text{ s}^{-1}$). These data and equations (1) – (7) allowed one to obtain the η/η_m versus $r_{\text{Ag}}^{\text{eff}}/r_{\text{RBC}}$ and $\dot{\gamma}_{\text{fin}}$ dependence plotted in Fig. 5.³ This three dimensional plot was used to determine the steady-state viscosity of RBC suspension

where aggregates with a certain effective size are formed at a given shear rate.

Discussion

Representative $\ln(r_{\text{Ag}}^{\text{eff}}/r_{\text{RBC}})$ versus $\ln(\tau/\eta_m)$ dependencies for suspensions with the external media containing D76 and D298 are shown in Fig. 6. The lowest ionic strength of the external media with D76 where the aggregation is still observed, is 0.06 M (20% saline + 80% LIS), whereas in suspensions with the D298 containing media RBCs form aggregates at I from 0.154 (100% saline) to 0.036 M (100% LIS). Following the lead of the study by Snabre et al. (1987), the critical values of τ/η_m for each ionic strength were determined by extrapolation of the linear portions of these curves to $\ln(r_{\text{Ag}}^{\text{eff}}/r_{\text{RBC}}) = 0$ (Fig. 6).

The dependencies of τ_c/η_m on the ionic strength for the suspensions with D76 and D298 containing media are plotted in Fig. 7. As shown above (see Introduction), non-monotonous shapes of these curves disagree with the depletion model and are consistent with the prediction of the bridging mechanism. A common feature of these dependencies is a plateau step at intermediate values of I . This plateau is extended over a larger range of ionic strengths for suspensions with the higher MW dextran.

This finding may be explained as follows: Dextran molecules consist of n -number of α -D-glucopyranose rings linked by glycosidic bonds. The enthalpic component of the dextran elasticity which was manifested by a plateau step in force-extension curves (Li et al. 1999; Marszalek et al. 1998; Rief et al. 1998), was accounted for by the chair-boat transition of the glucopyranose rings (Marszalek et al. 1998). These results allow the suggestion that a contribution of the enthalpic component to the dextran elasticity and hence a length of plateau must correlate positively with the number of pyranose rings or, in other words, with MW

³ Since D250 was not available at our laboratory, it was assumed that eqs. 5 and 6 obtained for suspensions with D250 describe adequately the shear dependent viscosity of suspensions with D298 which were used to measure the effective steady-state radius of RBC aggregates at different shear rates. Note that literature reports point out that this difference of molecular weights does not measurably affect both RBC aggregation and blood viscosity (Armstrong et al. 2004).

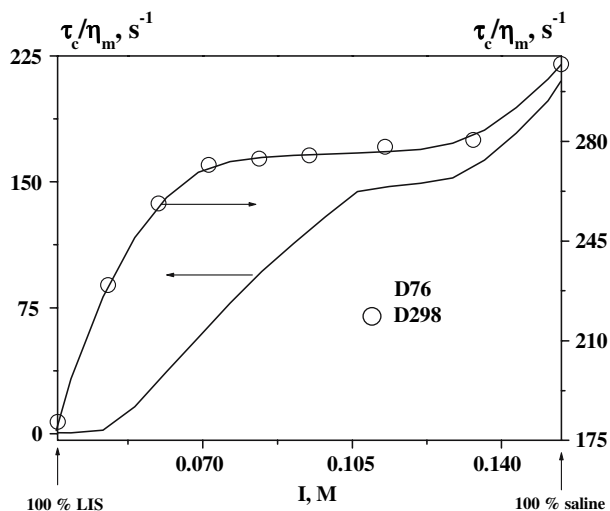


Fig. 7 The dependencies of τ_c/η_m on the ionic strength for suspensions with the external media containing D76 (23 g/l) and D298 (10 g/l)

of dextran. The results shown in Fig. 7 support this suggestion and thus, provide an additional argument for the bridging model of RBC aggregation.

Acknowledgments We wish to express our sincere gratitude to Prof. H. J. Meiselman from the University of Southern California (USA) for providing the shear viscosity data. This study was supported by a grant from the Israel Science Foundation, No. 457/02.

References

- Alvarez FJ, Herraez A, Tejedor MC, Diez JC (1996) Behavior of isolated rat and human red blood cells upon hypotonic-dialysis encapsulation of carbonic anhydrase and dextran. *Biotechnol Appl Biochem* 23:173–179
- Armstrong JK, Wenby RB, Meiselman HJ, Fisher TC (2004) The hydrodynamic radii of macromolecules and their effect on red blood cell aggregation. *Biophys J* 87:4259–4270
- Barshtein G, Tamir I, Yedgar S (1998) Red blood cell rouleaux formation in dextran solution: dependence on polymer conformation. *Eur Biophys J* 27:177–181
- Baskurt OK, Tugral E, Neu B, Meiselman HJ (2002) Particle electrophoresis as a tool to understand the aggregation behavior of red blood cells. *Electrophoresis* 23:2103–2109
- Bäumler H, Neu B, Iovtchev S, Budde A, Kiesewetter H, Latza R, Donath E (1999) Electroosmosis and polymer depletion layers near surface conducting particles are detectable by low frequency electrorotation. *Colloids Surf A: Physicochem Eng Aspects* 149:389–396
- Bäumler H, Donath E, Krabi A, Budde A, Kiesewetter H (2001) Electrophoresis of human red blood cells and platelets. Evidence for depletion of dextran. *Biorheology* 33:333–351
- Berezina TL, Sergey B, Zaets SB, Morgan C, Spillert CR (2002) Influence of storage on red blood cell rheological properties. *J Surg Res* 102:6–12
- Brooks DE (1973a) The effect of neutral polymers on the electrokinetic potential of cells and other charged particles:

- II. A model for the effect of adsorbed polymer on the diffuse double layer. *J Colloid Interface Sci* 43:687–699
- Brooks DE (1973b) The effect of neutral polymers on the electrokinetic potential of cells and other charged particles: III. Experimental studies on the dextran/erythrocyte system. *J Colloid Interface Sci* 43:700–713
- Brooks DE (1973c) The effect of neutral polymers on the electrokinetic potential of cells and other charged particles: IV. Electrostatic effects in dextran-mediated cellular interactions. *J Colloid Interface Sci* 43:714–726
- Brooks DE, Greig RG, Janzen J (1980) Mechanisms of erythrocyte aggregation. In: Cokelet GR, Meiselman HJ, Brooks DE (eds) *Erythrocyte mechanics and blood flow*. A.R. Liss, New York, pp 119–140
- Chien S, Simchon S, Abbot RE, Jan K-M (1977) Surface adsorption of dextrans on human red cell membrane. *J Colloid Interface Sci* 62:461–470
- Cicha I, Suzuki Y, Tateishi N, Shiba M, Muraoka M, Tadokoro K, Maeda N (2000) Gamma-ray-irradiated red blood cells stored in mannitol-adenine-phosphate medium: rheological evaluation and susceptibility to oxidative stress. *Vox Sang* 79:75–82
- Cokelet GR (1999) Viscometric, in vitro and in vivo blood viscosity relationships: how are they related? *Biorheology* 36:343–358
- Cudd A, Arvinte T, Schulz B, Nicolau C (1989) Dextran protection of erythrocytes from low-pH-induced hemolysis. *FEBS Lett* 250:293–296
- Derjaguin BV, Muller VM, Toporov YuP (1975) Effect of contact deformations on the adhesion of particles. *J Colloid Interface Sci* 53:314–326
- Donath E, Voigt A (1986) Electrophoretic mobility of human erythrocytes. On the applicability of the charged layer model. *Biophys J* 49:493–499
- Einstein A (1906) Eine neue bestimmung der molekul dimension. *Ann Phys* 19:289–306
- Fåhræus R (1929) The suspension stability of blood. *Physiol Rev* 9:241–274
- Fisher TE, Marszalek PE, Oberhauser AF, Carrion-Vazquez M, Fernandez JM (1999) The micro-mechanics of single molecule studied with atomic force microscopy. *J Physiol (Lond)* 520:5–14
- Fricke K, Wirthensohn K, Laxhuber R, Sackmann E (1986) Flicker spectroscopy of erythrocytes. A sensitive method to study subtle changes of membrane bending stiffness. *Eur Biophys J* 14:67–81
- Godin C, Caprani A (1997) Effect of blood storage on erythrocyte/wall interactions: implications for surface charge and rigidity. *Eur Biophys J* 26:175–82
- Goldsmith HL (1974) The microrheology of human erythrocyte suspensions. In *Proceedings of the 13th International Congress on Theoretical and Applied Mechanics*. Springer, Berlin, Heidelberg, New York, pp 85–103
- Haydon DA, Seaman GV (1967) Electrokinetic studies on the ultrastructure of the human erythrocyte. I. Electrophoresis at high ionic strengths—the cell as a polyanion. *Arch Biochem Biophys* 122:126–136
- Helfrich W (1978) Steric interaction of fluid membranes in multilayer systems. *Z Naturforsch* 33c:305–315
- Hovav T, Yedgar S, Manny N, Barshtein G (1999) Alteration of red cell aggregability and shape during blood storage. *Transfusion* 39:277–81
- Hsu J-P, Lin S-H, Tseng S (2003) Effect of cell membrane structure of human erythrocyte on its electrophoresis. *Colloids Surf B: Biointerfaces* 32:203–212

- de Kerchove AJ, Elimelech M (2005) Relevance of electrokinetic theory for “soft” particles to bacterial cells: implications for bacterial adhesion. *Langmuir* 21:6462–6472
- Krieger JM, Dougherty T (1959) A mechanism for non-Newtonian flow in suspensions of rigid spheres. *Trans Soc Rheol* 3:137–152
- Levine S, Levine M, Sharp KA, Brooks DE (1983) Theory of the electrokinetic behavior of human erythrocytes. *Biophys J* 42:127–135
- Li H, Rief M, Oesterhelt F, Glaub HE (1999) Force spectroscopy on single xanthan molecules. *Appl Phys A* 68:407–410
- Maeda N, Seike M, Suzuki Y, Shiga T (1988) Effect of pH on the velocity of erythrocyte aggregation. *Biorheology* 25:25–30
- Marszalek P, Oberhauser AF, Pang Y-P, Fernandez JM (1998) Polysaccharide elasticity governed by chair-boat transitions of the glucopyranose ring. *Nature* 396:661–664
- Marszalek P, Li H, Oberhauser AF, Fernandez JM (2002) Chair-boat transitions in single polysaccharide molecules observed with force-ramp AFM. *PNAS* 99:4278–4283
- Merrill EW, Benis AM, Gilliland ER, Sherwood TK, Salzman EW (1965) Pressure-flow relations of human blood in hollow fibers at low flow rates. *J Appl Physiol* 20:954–967
- Mi XQ, Chen JY, Cen Y, Liang ZJ, Zhou LW (2004) A comparative study of 632.8 and 532 nm laser irradiation on some rheological factors in human blood in vitro. *J Photochem Photobiol B* 74:7–12
- Neu B, Meiselman HJ (2002) Depletion-mediated red blood cell aggregation in polymer solutions. *Biophys J* 83:2482–2490
- Neu B, Sowemimo-Coker SO, Meiselman HJ (2003) Cell-cell affinity of senescent human erythrocytes. *Biophys J* 85:75–84
- Ohshima H (2000) On the general expression for the electrophoretic mobility of a soft particle. *J Colloid Interface Sci* 228:190–193
- Pribush A, Meiselman HJ, Meyerstein D, Meyerstein N (1999) Dielectric approach to the investigation of erythrocyte aggregation: I. Experimental basis of the method. *Biorheology* 36:411–423
- Pribush A, Meiselman HJ, Meyerstein D, Meyerstein N (2000) Dielectric approach to investigation of erythrocyte aggregation. II. Kinetics of erythrocyte aggregation-disaggregation in quiescent and flowing blood. *Biorheology* 37:429–441
- Pribush A, Meyerstein D, Meyerstein N (2004a) Conductometric study of shear-dependent processes in red cell suspensions. I. Effect of red blood cell aggregate morphology on blood conductance. *Biorheology* 41:13–28
- Pribush A, Meyerstein D, Meyerstein N (2004b) Conductometric study of shear-dependent processes in red cell suspensions. II. Transient cross-stream hematocrit distribution. *Biorheology* 41:29–43
- Quemada D (1977) Rheology of concentrated disperse systems and minimum energy dissipation principle. I: Viscosity-concentration relation. *Rheol Acta* 16:82–94
- Raat NJ, Verhoeven AJ, Mik EG, Gouwerok CW, Verhaar R, Goedhart PT, de Korte D, Ince C (2005) The effect of storage time of human red cells on intestinal microcirculatory oxygenation in a rat isovolemic exchange model. *Crit Care Med* 33:39–45
- Rampling MW (1988) Red cell aggregation and yield stress. In: Lowe GDO (ed) *Clinical Blood Rheology*. CRC Press, Boca Raton, pp 45–64
- Rief M, Oesterhelt F, Heyman B, Gaub H (1997) Single molecule force spectroscopy on polysaccharides by atomic force microscopy. *Science* 275:1295–1297
- Rief M, Fernandez JM, Gaub HE (1998) Elastically coupled two-level systems as a model for biopolymer extensibility. *Phys Rev Lett* 81:4764–4767
- Schwan HP (1963) Determination of biological impedances. In: Nastuk WL (ed) *Physical techniques in biological research*, vol. 6, Academic Press, New York, p 344
- Snabre P, Bitbol M, Mills P (1987) Cell disaggregation behavior in shear flow. *Biophys J* 51:795–807
- Snabre P, Haider L, Boynard M (2000) Ultrasound and light scattering from a suspension of reversible fractal clusters in shear flow. *Eur Phys J E* 1:41–53
- Sonntag RC, Russel WB (1986) Structure and breakup of flocs subjected to fluid stresses: I. Shear experiments. *J Colloid Interface Sci* 113:399–413
- Sonntag RC, Russel WB (1987) Structure and breakup of flocs subjected to fluid stresses: II. Theory. *J Colloid Interface Sci* 115:378–389
- Starov VM, Zhdanov VG (2003) Viscosity of emulsions: influence of flocculation. *J Colloid Interface Sci* 258:404–414
- Thurston GB (1972) Viscoelasticity of human blood. *Biophys J* 12:1205–1217
- Yeow YL, Wickramasinghe SR, Leong YK, Han B (2002) Model-independent relationships between hematocrit, blood viscosity, and yield stress derived from Couette viscometry data. *Biotechnol Prog* 18:1068–1075